Journal of Sleep Research

RESEARCH ARTICLE OPEN ACCESS

An Electroencephalographic Study of Sleep Spindle and Infraslow Oscillation in Children With Autism Spectrum Disorder

Kevin Liu[1] | Binbin Sun[2] | Bryan K. Wang[3] | Jonathan Chen[3,4] | M. Brandon Westover[5] | Fu-Ying Tian[2] | Haoqi Sun[5] | Xue-Jun Kong[1,3,6]

[1]Fetal-Neonatal Neuroimaging and Developmental Science Center, Boston Children's Hospital, Boston, Massachusetts, USA | [2]Shenzhen Maternity and Child Healthcare Hospital, Women and Children's Medical Center, Southern Medical University, Shenzhen, Guangdong, China | [3]Athinoula A. Martinos Center for Biomedical Imaging, Massachusetts General Hospital, Charlestown, Massachusetts, USA | [4]University of Pittsburgh, Pittsburgh, Pennsylvania, USA | [5]Department of Neurology, Beth Israel Deaconess Medical Center, Boston, Massachusetts, USA | [6]Department of Medicine and Psychiatry, Beth Israel Deaconess Medical Center, Boston, Massachusetts, USA

Correspondence: Haoqi Sun (hsun3@bidmc.harvard.edu) | Xue-Jun Kong (june.kong@childrens.harvard.edu)

Received: 9 September 2025 | **Revised:** 11 December 2025 | **Accepted:** 28 January 2026

Keywords: autism | infraslow oscillations | sleep electrophysiology | slow oscillations | spindle

ABSTRACT

We investigated whether sleep microstructures show spatial differences in young children with autism compared with typically developing peers. 32-channel electroencephalography (EEG) during natural sleep after 5–6 h of partial sleep deprivation was recorded from 53 children (26 with autism, 27 typically developing; 1.1–5.1 years). Quantified EEG features included spindle density, frequency, morphology, slow oscillations and the relative power of infraslow oscillations (0.005–0.03 Hz). Clinical associations were examined using the Autism Diagnostic Observation Schedule, the Childhood Autism Rating Scale and the Gesell Developmental Schedules. Children with autism showed greater modulation of spindle frequency by the phase of slow oscillations at a right frontal scalp electrode (F8). An infraslow peak slightly below 0.02 Hz was present in both groups. Although group differences in infraslow power did not remain significant after correction for multiple comparisons, infraslow power correlated positively with autism severity in males, over posterior and temporal regions. These findings indicate that sleep microstructures in early childhood reflect thalamocortical and cortical dysfunction with sex-specific clinical associations.

1 | Introduction

Autism spectrum disorder (ASD) is a fast-growing neurodevelopmental condition characterised by persistent deficits in social communication and the presence of restricted, repetitive behaviours (American-Psychiatric-Association 2013). According to recent estimates, approximately 1 in 31 children in the United States is diagnosed with ASD (Shaw et al. 2025), with incidence rates continuing to rise. ASD is a highly heterogeneous disorder with no definitive cure and a complex, multifactorial aetiology. Altered brain functional connectivity and imbalances in excitatory and inhibitory signalling, particularly involving glutamatergic and GABAergic circuits, have been implicated in its pathophysiology (Gao and Penzes 2015; Jiang et al. 2022).

Sleep disturbances are highly prevalent in ASD, with 60%–90% of individuals experiencing disturbances such as chronic insomnia, fragmented sleep, or reduced sleep duration (Arazi et al. 2019). Comprehensive reviews have emphasised that sleep problems in ASD are pervasive across childhood, often involving difficulties with sleep onset and maintenance, atypical sleep architecture and altered arousal regulation (Moore

Kevin Liu and Binbin Sun contributed equally to this manuscript.

et al. 2017; Souders et al. 2017). Polysomnography (PSG) and other objective sleep measures have consistently demonstrated abnormalities in NREM sleep organisation and arousal regulation in ASD, complementing parent-reported measures that frequently underestimate physiological disturbances (Moore et al. 2017).

In contrast to the hypnogram-derived macrostructures such as sleep duration, the sleep EEG microstructures directly reflect brain functions, including synaptic homeostasis, memory consolidation and mood regulation, and therefore contain rich information about brain health (Fjell and Walhovd 2025; Palmer and Alfano 2017; Tononi and Cirelli 2006; Walker and Stickgold 2004). Many studies have found differences in sleep EEG microstructures in children with ASD (Cumming et al. 2024; Kawahara et al. 2022). For example, sleep spindle (brief bursts of 11–15 Hz activity) during non-rapid eye movement (NREM) sleep is a result of thalamocortical interaction (Herrera and Tarokh 2024). The spindle–slow oscillation (SO) coupling has been associated with memory consolidation (Bastian et al. 2022; Ng et al. 2025). In a preliminary study, overall spindle density is lower, with spindles more distributed in N3 than in N2, based on 28 children aged 4–10 years (Kawahara et al. 2022). Recent findings also indicate that spindle chirp (frequency deceleration) is faster (more negative) in 121 children aged 1–8 years (Cumming et al. 2024). However, the spatial distribution of spindle deficits remains unknown, due to the limited number of EEG electrodes in previous studies. On the other hand, during NREM sleep, the sigma band power timeseries shows rhythmic fluctuations at infraslow frequencies (~0.02 Hz), consistent with established descriptions of infraslow modulation of spindle activity, which has been connected to the norepinephrine system and glymphatic clearance in mice, a process impaired in neurodegenerative diseases in the older population but understudied in the paediatric population (Hauglund et al. 2025; Lord et al. 1994, 2000; Martin et al. 2013; Osorio-Forero et al. 2025; Purcell et al. 2017; Sun et al. 2023).

Here, we investigate the sleep microstructure of children at 1–5 years old with ASD and typically developing (TD) children using 32-channel EEG after partial sleep deprivation to address the current gaps in understanding spindle, SO and ISO abnormalities in early ASD. We hypothesize that children with ASD would show alterations in spindle characteristics, SO-spindle coupling and ISO strength compared with TD children, and that these features would relate to clinical assessments.

2 | Methods

2.1 | Participants and Clinical Assessments

The study was approved by the Research Ethics Committee of Shenzhen Maternal and Child Healthcare Hospital (SFYLS [2022]026). All participants were recruited from Shenzhen, China, including children diagnosed with ASD and TD children. A total of 64 children were initially recruited for participation in this study. Of these, 11 were excluded prior to analysis due to missing demographic information ($n = 2$) or absence of recorded sleep during the EEG session ($n = 9$), resulting in a final analytic sample of 53 children. The analysed cohort consisted of 26 children diagnosed with ASD (6 females, 20 males) and 27 TD children (8 females, 19 males). The ages of participants included in the final sample ranged from 1.1 to 5.1 years. Parents or legal guardians of all participants were informed that the study procedures adhered to ethical guidelines and posed no known physiological or psychological risks. Written informed consent was obtained prior to participation. Upon completion of the study visit, participants received a gift card as compensation.

ASD diagnoses were established according to DSM-5 criteria by specialist paediatric psychiatrists and developmental-behavioural clinicians (American-Psychiatric-Association 2013). Diagnostic evaluation incorporated the Autism Diagnostic Observation Schedule (ADOS; Modules 1 or 3, depending on expressive language ability), the Autism Diagnostic Interview-Revised (ADI-R) and clinical judgement based on direct behavioural observation (Lord et al. 1994, 2000). The Childhood Autism Rating Scale (CARS) was also administered as an additional measure of autism symptom severity (Schopler et al. 1980). Higher ADOS and CARS scores reflect greater autism symptom severity. For children younger than 18 months who screened positive on early behavioural risk markers, diagnosis was made by a multidisciplinary team (child psychiatrists, developmental paediatricians and psychologists) using ADOS-based observational assessment, ADI-R caregiver interviews and exclusion of alternative neurodevelopmental or sensory disorders. General developmental level was assessed with the Gesell Developmental Schedules (GDS), which provide developmental quotients across functional domains but are not diagnostic for ASD (Gesell and Amatruda 1945).

TD status was defined through a multi-step screening protocol. Children were required to have a GDS developmental quotient greater than 85, confirmed by medical records obtained within 6 months of EEG assessment (TD range: 89–110). All TD participants also previously completed the Denver Developmental Screening Test, with results indicating age-appropriate development (Frankenburg and Dodds 1967). To prevent inclusion of ASD cases with normal developmental quotients, TD classification additionally required: (1) absence of ASD core symptoms based on clinician examination; (2) a negative ADI-R parent interview; and (3) confirmation from caregivers that developmental milestones and social-communication behaviours followed typical trajectories.

Exclusion criteria applied to both ASD and TD participants included: (1) known metabolic, neurogenetic, or neurological disorders (e.g., cerebral palsy, seizure history); (2) neurodevelopmental conditions other than ASD (e.g., attention-deficit/hyperactivity disorder); (3) primary sleep disorders that could interfere with EEG quality (e.g., sleep apnea, severe insomnia, frequent night awakenings), as determined by caregiver interview and review of medical records; and (4) current use of medications affecting sleep or arousal (e.g., melatonin, sedatives, psychotropic medications). ASD itself was not an exclusion, but

ASD participants with comorbid severe sleep disorders requiring pharmacologic treatment were excluded per study protocol.

2.2 | EEG Data Acquisition and Preprocessing

Electroencephalography (EEG) data were acquired using a 32-lead HydroCel Geodesic Sensor Net connected to a NetAmps 300 amplifier system (Electrical Geodesics Inc.) at a sampling rate of 250 Hz, referenced to Cz. The channels were mapped to the standard 10–20 system using the manufacturer's lookup table. All EEG data were recorded between 9:00 AM and 3:00 PM to ensure consistency in the recording environment. EEG sessions lasted between 1 and 1.5 h and were conducted following a 5–6 h period of partial sleep deprivation to facilitate natural sleep without sedation or hypnosis (Peltola et al. 2023). Signals were preprocessed using MNE version 1.5.1, including notch filtering at 50 Hz to remove electrical line noise and subsequent bandpass filtering between 0.3 and 35 Hz to remove slow drifts and high-frequency noise. The filter type was finite impulse response (FIR), with a non-causal zero phase based on a symmetric impulse response. EEG recordings were segmented into consecutive 30-s epochs. Sleep staging was performed manually in 30-s epochs following standard American Academy of Sleep Medicine (AASM) paediatric scoring guidelines (Berry et al. 2012). Trained scorers annotated Wake, NREM, REM, abnormal and artefact epochs with independent review. The abnormal and artefact epochs were excluded from the analysis (Campbell 2009). Only NREM sleep epochs were used for spindle, SO and ISO analyses. Sleep architecture (total sleep time, NREM duration, REM duration, wake duration and abnormal epochs) is summarised in Table 1.

2.3 | Spindle and SO Detection

Sleep spindles and SOs were detected using the open-source software Luna version 0.99 (https://zzz.bwh.harvard.edu/luna/). Analyses included EEG features derived from a total of 27 scalp channels: the 19 standard electrodes of the international 10-20 system (Fp1, Fp2, F3, F4, C3, C4, P3, P4, O1, O2, F7, F8, T7, T8, P7, P8, Fz, Pz, Oz) as well as eight additional scalp channels: above M1, above M2, between P7-T7, between P8-T8, between P7-O1, between P8-O2, between nasion-Fz and between Cz-Fz. Non-scalp channels were excluded from analysis.

Spindles were detected using wavelet transformation with a multiplicative threshold of 4.5 and a cycle number of 7 at NREM sleep. To account for variability in spindle frequency among children, detection was conducted across all frequencies in the broad sigma range (10.5–15.5 Hz, step size 0.5 Hz) and then combined based on temporal overlap within each channel. To

TABLE 1 | Summary of participant demographics, clinical characteristics and sleep architecture, stratified by group and sex.

	ASD cohort ($n=26$)		TD cohort ($n=27$)	
Mean (SD)	**Male ($n=20$)**	**Female ($n=6$)**	**Male ($n=19$)**	**Female ($n=8$)**
Age (years) [min-max]	3.1 (1.2) [1.06–5.1]	3.2 (1.3) [2.05–5.07]	2.7 (1.1) [1.05–5.01]	2.4 (1.3) [1.05–4.09]
Total sleep time (hours)	1.19 (0.18)	1.21 (0.13)	1.26 (0.22)	1.19 (0.27)
NREM time (hours)	0.73 (0.20)	0.69 (0.13)	0.88 (0.30)	0.70 (0.28)
REM time (hours)	0.02 (0.05)	0.11 (0.20)	0.02 (0.05)	0.03 (0.06)
Wake time (hours)	0.41 (0.24)	0.39 (0.13)	0.33 (0.18)	0.40 (0.29)
Abnormal time (hours, possible epileptic)	0.04 (0.07)	0.03 (0.04)	0.03 (0.05)	0.06 (0.11)
CARS Score	33.9 (3.3)	35.3 (3.4)	—	—
Autism diagnostic observation schedule (ADOS)				
Total score	13.8 (3.1)	15.2 (3.1)	—	—
Communication	5.6 (1.4)	6.3 (1.0)	—	—
Interactivity	8.2 (2.4)	8.8 (2.0)	—	—
Gesell developmental schedules (GDS)				
Adaptive behaviour	57.8 (9.9)	52.3 (8.6)	—	—
Gross motor	64.7 (11.6)	67.2 (14.1)	—	—
Fine motor	61.6 (12.9)	52.3 (12.1)	—	—
Language	47.5 (10.6)	41.5 (9.7)	—	—
Personal-social	50.7 (7.8)	50.2 (7.5)	—	—

establish an optimal detection quality threshold, we initially applied a relaxed threshold ($q = 0$ in Luna), followed by a manual review of 786 randomly selected spindle candidates to classify events as true spindles or false detections. An optimal quality threshold ($q = 0.53$) was selected based on Youden's J statistic derived from the receiver operating characteristic (ROC) analysis, yielding a sensitivity (recall) of 0.71, specificity of 0.58, precision of 0.43, an F1 score of 0.54 and Cohen's kappa coefficient of 0.24 (Figure S1). Spindle detection was then re-run using this optimised threshold for subsequent analyses.

Spindle metrics calculated included density (number per minute of NREM sleep), amplitude (uV), duration (second), integrated spindle activity (ISA), spindle frequency (Hz), number of oscillations per spindle, chirp (log ratio of mean peak-to-peak time intervals in the first versus the second half of a spindle) and morphological symmetry (spindle trough-based centre location). We did not separate fast and slow spindles because the separation frequency is unclear at a young age (McClain et al. 2016; Sun et al. 2023).

SOs were identified by band-pass filtering EEG signals between 0.5 and 4 Hz, detecting zero-crossings, and retaining oscillations with durations between 0.8 and 2.0 s, negative-peak and peak-to-peak amplitudes greater than three times the median amplitude. SO metrics included peak-to-peak amplitude, duration, rate and slope. Spindle–SO coupling was quantified as the proportion of spindles temporally overlapping (any overlap in time) with SOs, SO-coupled spindle density (number per minute of NREM sleep) and SO-phase-dependent spindle frequency modulation (circular-linear correlation between spindle instantaneous frequency and SO phase), where the former two reflect temporal co-occurrence, and the latter captures phase-specific coupling.

2.4 | Infraslow Oscillation (ISO) Analysis

ISO spectral analyses were based on Lázár et al. (2019). The analyses were performed on artefact-free continuous NREM epochs. EEG signals were segmented into overlapping epochs of 4 s with a step size of 2 s. Sigma-band (11–15 Hz) power spectral densities were computed using the multitaper method, converted to a logarithmic scale (dB) and resampled at 0.5 Hz. To characterise the rhythm of sigma-band power in the infraslow frequency range (0.001–0.1 Hz), sigma-band power time series were segmented into longer epochs (256-s windows, 64-s step size), detrended and analysed using the multitaper method. Relative ISO band power was computed as the area under the sigma-band power curve from 0.005 to 0.03 Hz divided by the total sigma-band power from 0.001 to 0.1 Hz, expressed as a percentage. Peak ISO frequencies were also extracted for each channel.

2.5 | Statistical Analysis

Statistical analyses were conducted using R (version 4.3.2). Participants with substantial missing EEG data were excluded to ensure data quality due to no sleep captured during recording. Specifically, for ISO features, participants with more than 50% missing data were excluded ($n = 4$). For sleep spindle features, participants with over 15% missing data were excluded ($n = 7$). These missingness thresholds were chosen based on the distribution of missing data in each dataset, which showed clear separation between participants with minimal missingness and those with extensive data loss. Features with greater than 20% missing data across participants were removed. There were 965 sleep microstructure variables for analysis. The remaining missing values were imputed using median values calculated separately within the ASD and TD groups.

Analysis of covariance (ANCOVA) models was tested for sex-dependence of EEG features using a group-by-sex interaction term (EEG feature ~ group + age + sex + group × sex). The main effects of the group were subsequently evaluated for all EEG-derived features using ANCOVA, adjusting for age and sex as covariates. All analyses uniformly applied a main-effects ANCOVA approach to maintain methodological consistency and maximise statistical power. Considering the exploratory nature and high dimensionality of our EEG feature set, principal component analysis (PCA)-based Bonferroni correction was chosen as the most appropriate method to control for Type I error. Specifically, the effective number of independent tests was defined as the minimum number of principal components required to explain at least 99% of the total variance. For comparison of sleep microstructure features, the effective number of comparisons was 48, with a corrected significance threshold of $p = 0.00104$; for comparison of ISO relative power, the number of effective comparisons was 19 with a corrected significance threshold of $p = 0.00263$. Significant group differences in sleep microstructure features and relative ISO band power were visualised using topographical maps to illustrate spatial distributions and highlight EEG channels meeting PCA-based Bonferroni significance thresholds. Channel-wise peak ISO frequency and peak ISO power were extracted for each participant, averaged across channels and analysed using linear models with diagnostic group, age and sex as predictors.

Exploratory EEG-clinical correlation analyses were stratified by sex to examine whether associations differed between males and females, as suggested by prior research (Lai et al. 2015; McFayden et al. 2023; Werling and Geschwind 2013). Within the ASD group, Pearson correlation analyses were performed separately by sex to examine relationships between significant sleep microstructure features, relative ISO band power and clinical ASD severity measures. To formally test whether the correlation coefficients differed between sexes, we compared male and female correlations using Fisher's r-to-z transformation, yielding a two-sided p value for the difference. These p values were used only to evaluate sex differences in correlation strength and were not corrected for multiple comparisons due to the exploratory nature of this analysis. Statistical significance was set at $\alpha < 0.05$ (uncorrected). All confidence intervals were at 95%. Because these analyses were exploratory and primarily intended to visualise potential sex-specific patterns rather than establish adjusted effect estimates, correlations were computed without additional covariate adjustment. Analyses involving relative ISO and ASD clinical severity measures were conducted only in ASD males because clinical severity measures were exclusively available in the ASD cohort, and the ASD female subsample ($n = 6$) was insufficient for reliable correlation estimation.

2.6 | Data and Code Availability

All codes used to generate figures, tables and intermediate results in this manuscript are publicly available on GitHub (https://github.com/kevinliu-bmb/eeg_sleep_spindle_iso). The dataset supporting the conclusions of this study can be made available upon reasonable request from the corresponding author.

3 | Results

3.1 | Cohort Characteristics

The 53 subjects included in the analysis consist of 6 ASD females, 20 ASD males, 8 TD females and 19 TD males. The age range is 1.1–5.1 years. A detailed cohort selection flowchart is presented in Figure 1. Table 1 summarises participant demographics, clinical characteristics and sleep architecture metrics of the final cohort stratified by group and sex. There were no significant differences in age or sex distribution between the ASD and TD groups. Clinical severity measures (ADOS, CARS and GDS) were available exclusively for the ASD cohort, reflecting the clinical assessments specific to autism diagnosis, whereas total sleep time and the durations of NREM, REM, wake and abnormal epochs are shown for both groups to contextualise the EEG data used for spindle and ISO analyses.

3.2 | Alterations in Sleep Spindles in ASD

All spindle, SO and spindle–SO coupling measures were tested for group differences using the same ANCOVA model (adjusting for age and sex). Among all features examined, only SO-phase-dependent spindle frequency modulation at EEG channel F8 (right frontal region) showed a significant group effect after PCA-based Bonferroni correction, with higher modulation in children with ASD compared to TD participants ($\beta = 0.232$, SE = 0.065, $t = 3.58$, $p = 0.000789$; Figure 2). For this modulation, both groups have positive values, indicating spindles accelerating along the SO. Meanwhile, the median SO coupling phase is 125 degrees, which is at the first half of the rising slope after the negative peak (90 degrees). Therefore, the ASD group has spindles that accelerate more rapidly at the rising slope of SOs. No other group-level differences in spindle, SO, or spindle–SO coupling indices reached statistical significance. Additionally, no significant group-by-sex interactions were detected.

Age was found to be negatively associated with mean ISA per spindle at EEG channels F4 and F7. Specifically, increased age was associated with reduced mean ISA per spindle (F4: $\beta = -0.153$, SE = 0.040, $p = 0.00035$; F7: $\beta = -0.141$, SE = 0.041, $p = 0.00104$), suggesting a developmental decline in this measure around 3 years old (Figure S2).

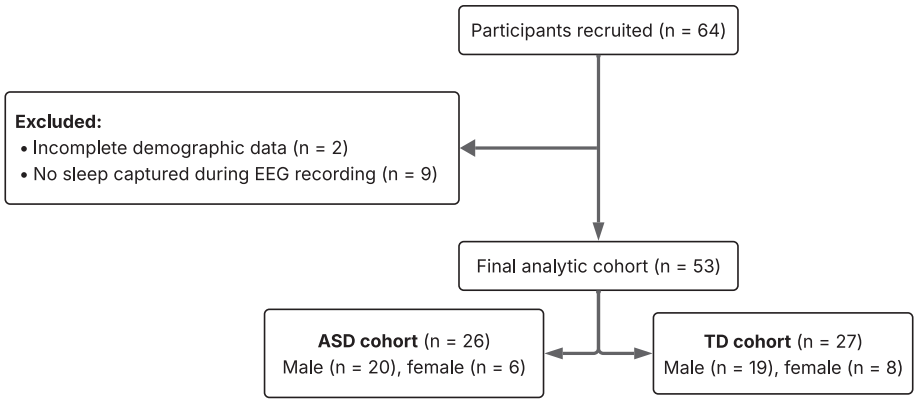

FIGURE 1 | Cohort flowchart. A total of 64 participants were initially recruited. The final analytic cohort comprised 53 participants (TD = 27, ASD = 26).

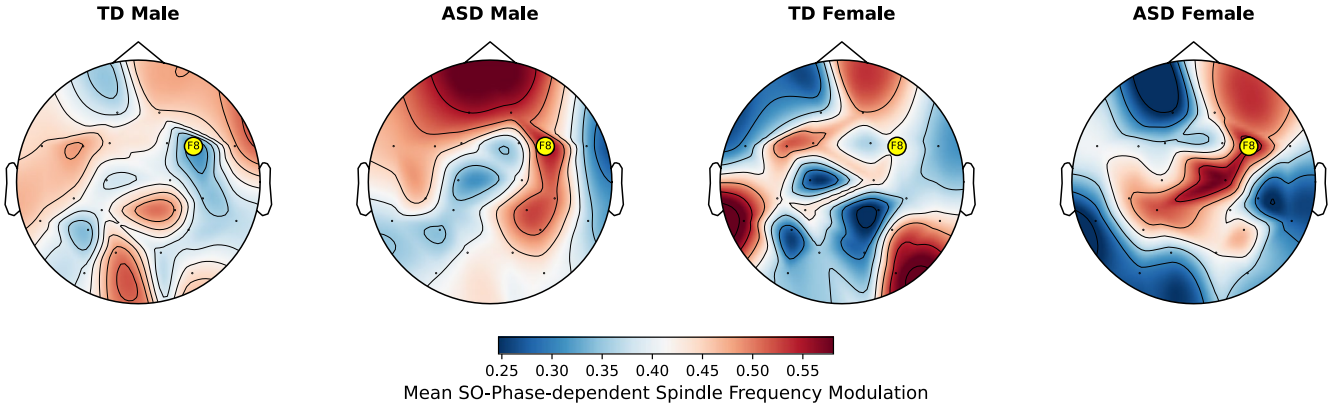

FIGURE 2 | Topographical maps of SO-phase-dependent spindle frequency modulation across EEG channels, stratified by group and sex. Each map displays the mean circular-linear correlation between slow oscillation (SO) phase and spindle instantaneous frequency for the indicated subgroup. Red shading indicates stronger modulation; blue shading indicates weaker modulation. The significant channel is marked with a gold circle.

3.3 | ISO Spectral Characteristics and Relative ISO Band Power

Spectral analyses showed a visually identifiable peak in sigma-power timeseries near ~0.02 Hz in both ASD and TD groups (Figure 3). Figure S3 illustrates representative channel-level ISO spectra from the youngest subjects, demonstrating that a comparable peak was observable across individual participants, including those as young as 1.05 years old. While a peak was visually apparent in both groups, linear models confirmed no significant differences in its frequency or amplitude between ASD and TD children (peak frequency: $\beta = -0.00013$, $p = 0.949$; peak power: $\beta = -0.00212$, $p = 0.346$).

ANCOVA models evaluating relative ISO band power (0.005–0.03 Hz) revealed no significant group-by-sex interactions across any scalp EEG channels after adjusting for age (all interaction terms $p > 0.05$). Similarly, the main effects of diagnostic group (adjusting for age and sex) did not reach significance after PCA-based Bonferroni correction.

Although no scalp channels demonstrated statistically significant group differences, we visualised the spatial distribution of relative ISO band power across the scalp using topographic maps (Figure 4), which revealed modest variation across regions but no systematic group-level differences.

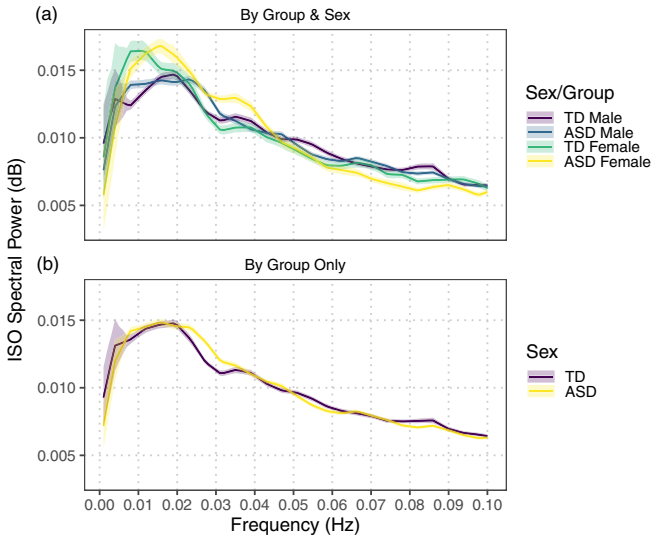

FIGURE 3 | Group-averaged ISO spectra. (a) Stratified by group and sex; (b) stratified by group only. Mean ISO spectra during non-rapid eye movement (NREM) sleep were calculated separately for male and female participants in ASD and TD groups. Shaded areas indicate 95% confidence intervals, visualising the variability and reliability of the group differences observed across the ISO frequency range.

3.4 | Sex-Stratified Associations Between Sleep EEG Features and Clinical Measures

We examined associations between sleep EEG microstructural features and clinical measures within the ASD group, stratified by sex (Figure 5; Table 2). Several spindle-related measures showed sex-specific patterns. In males, SO-phase-dependent spindle frequency modulation at F8 was positively associated with fine motor performance, and mean ISA per spindle at F4 was significantly correlated with both younger age and greater autism severity, including ADOS total and interactivity scores. In females, SO-phase-dependent spindle frequency modulation at F8 was strongly and negatively correlated with autism severity across multiple domains (ADOS total, communication and interactivity), and ISA per spindle at F7 was positively associated with language development. To visualise these associations despite the small sex-stratified sample sizes, we provide scatterplots for all significant correlations, displayed separately for males and females (Figure S4).

To determine whether these relationships differed significantly between sexes, we compared male and female correlation coefficients using Fisher's r-to-z transformation. Several associations involving SO-phase-dependent spindle frequency modulation at F8 differed significantly between sexes ($p < 0.05$; Table 2), confirming sex-specificity in these EEG-clinical relationships.

Exploratory analyses in males identified significant positive correlations between increased relative ISO power and higher autism severity measured by CARS total scores, across multiple

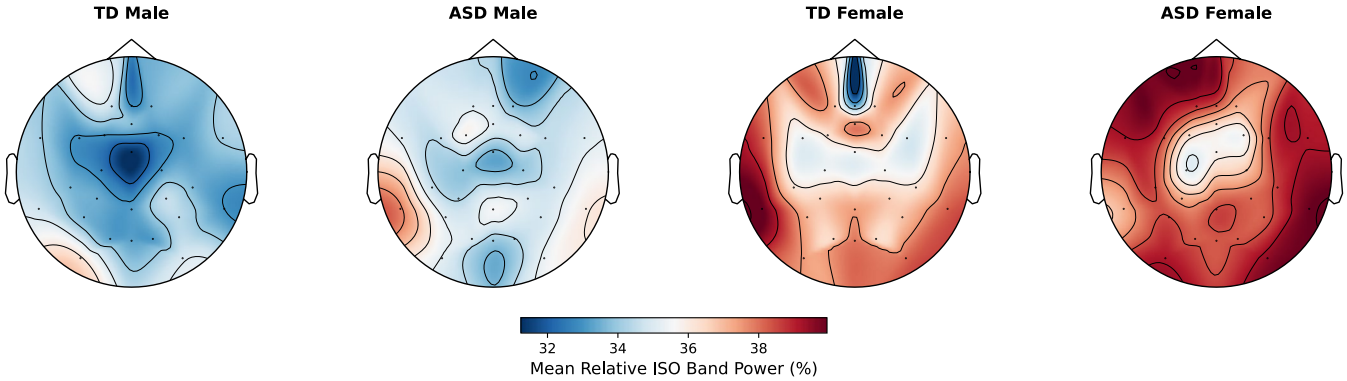

FIGURE 4 | Topography of relative ISO band power (0.005–0.03 Hz). Topographic maps display the spatial distribution of mean relative ISO band power across the scalp, stratified by diagnostic group and sex. Values reflect average spectral power in the 0.005–0.03 Hz band expressed as a percentage of the total sigma-band power. No channels showed statistically significant group differences after correction, but the figure highlights subtle, non-significant topographic differences across groups.

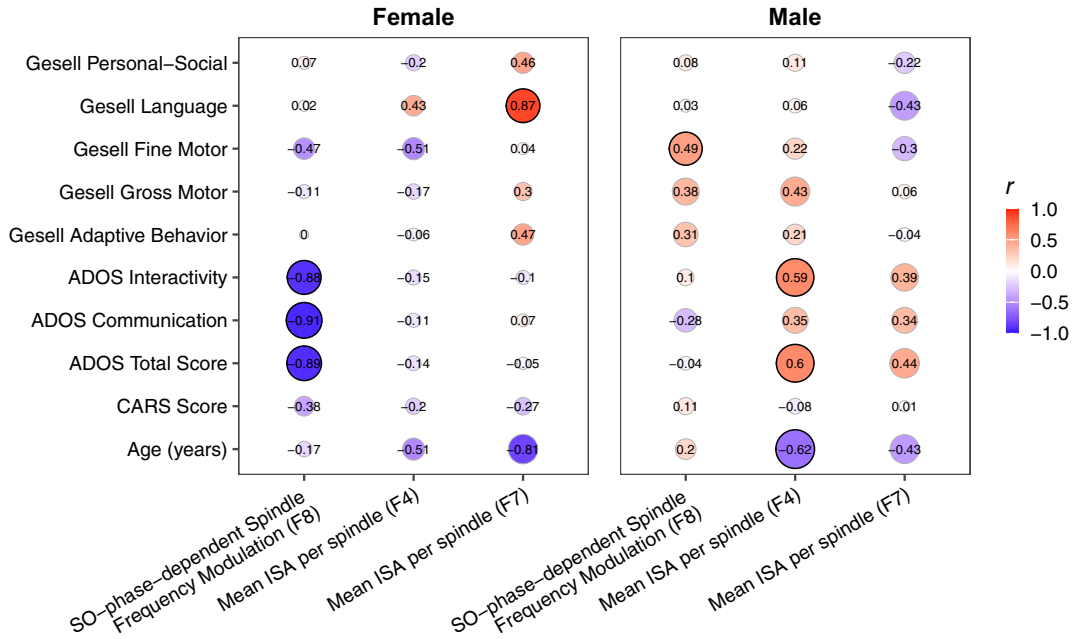

FIGURE 5 | Sex-specific correlations between clinical measures and selected EEG-derived sleep microstructure features in ASD. Pearson correlations between clinical severity measures and selected EEG features, including SO-phase-dependent spindle frequency modulation at channel F8, mean ISA per spindle at channel F4 and mean ISA per spindle at channel F7. Results are shown separately for females (left panel) and males (right panel). Circle colour indicates correlation strength (r; red: positive, blue: negative), while circle size represents statistical significance ($-\log_{10}[p]$). Significant correlations ($p < 0.05$, uncorrected) are outlined with bold black circles.

TABLE 2 | Sex-stratified correlations between EEG-derived sleep microstructure features and clinical measures in ASD, with Fisher r-to-z comparison between sexes.

		Male ($n = 20$)		Female ($n = 6$)		Fisher
Clinical feature	**EEG feature**	***r***	***p****	***r***	***p****	***r*-*z* *p***
ADOS total score	SO-phase-dependent Spindle Frequency Modulation (F8)	−0.0437	0.8548	−0.8927	**0.0166**	**0.0263**
ADOS communication		−0.2804	0.2311	−0.9113	**0.0115**	**0.0464**
ADOS interactivity		0.1022	0.6680	−0.8774	**0.0216**	**0.0191**
Gesell fine motor		0.4899	**0.0283**	−0.4748	0.3413	0.0929
Age (years)	Mean ISA per spindle (F4)	−0.6185	**0.0037**	−0.5094	0.3020	0.7975
ADOS total score		0.5976	**0.0054**	−0.1366	0.7963	0.1867
ADOS interactivity		0.5919	**0.0060**	−0.1497	0.7772	0.1843
Gesell language	Mean ISA per spindle (F7)	−0.4261	0.0610	0.8749	**0.0225**	**0.0039**

*Sex-stratified Pearson correlation p values (uncorrected). Bold represents $p < 0.05$.
**Two-sided p values from Fisher's r-to-z test comparing male and female correlation coefficients (uncorrected). Bold represents $p < 0.05$.

posterior and temporal scalp regions. These correlations were assessed only in ASD males due to insufficient sample size in ASD females and included channels P4 ($r = 0.46$, $p = 0.041$), O1 ($r = 0.50$, $p = 0.026$), O2 ($r = 0.57$, $p = 0.009$), F8 ($r = 0.59$, $p = 0.006$), T7 ($r = 0.46$, $p = 0.039$), T8 ($r = 0.65$, $p = 0.002$), P7 ($r = 0.49$, $p = 0.030$), P8 ($r = 0.69$, $p = 0.001$) and Oz ($r = 0.54$, $p = 0.014$), as well as extended scalp electrodes above M1 ($r = 0.55$, $p = 0.011$), above M2 ($r = 0.61$, $p = 0.005$), between P8-T8 ($r = 0.62$, $p = 0.003$) and between P7-O1 ($r = 0.49$, $p = 0.028$) (Figure 6; Table S1). Additionally, greater ISO power was associated with better fine motor function, as measured by GDS, at P3 ($r = 0.46$, $p = 0.041$) and Fz ($r = 0.46$, $p = 0.043$) in ASD males.

4 | Discussion

This study investigated sleep spindle characteristics, SOs and ISO in young children with and without ASD between 1.1 and 5.1 years of age. After adjusting for age and sex, we found that SO-phase-dependent modulation of spindle frequency at a right frontal EEG site (F8) was significantly higher in children with

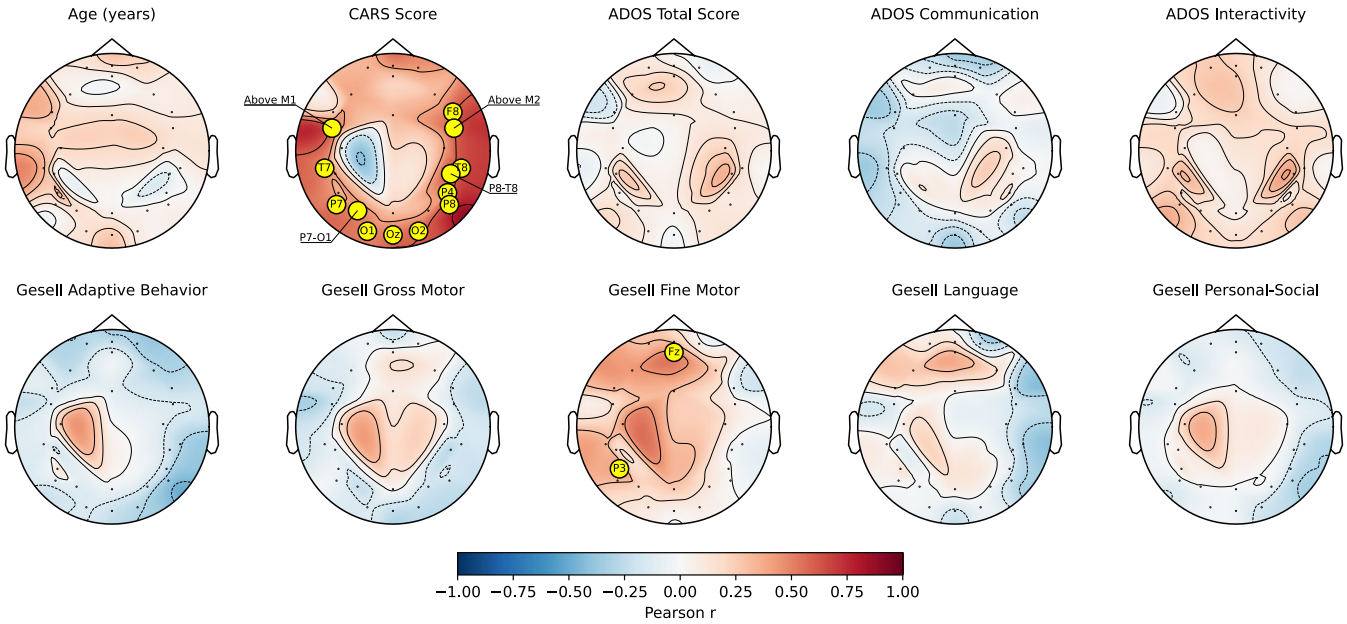

FIGURE 6 | Topographic distribution of correlations between clinical severity measures and relative ISO band power in males with ASD. Scalp topography maps display Pearson correlation coefficients (r) between relative ISO band power (0.005–0.03 Hz) and clinical scores in males diagnosed with ASD. Red and blue shading represent positive and negative correlations, respectively. Channel labels are shown only for electrodes with statistically significant correlations ($p < 0.05$, uncorrected), which are also marked with yellow circles.

ASD compared to TD peers. Sex-stratified analyses revealed several EEG-ASD clinical metric associations differed significantly between sexes and were driven primarily by strong negative correlations in females, particularly between SO-phase-dependent spindle frequency modulation at F8 and ADOS severity measures. Finally, both groups exhibited a visually identifiable peak near ~0.02 Hz, detectable even in children as young as 1 year old. Meanwhile, males showed significant positive correlations between ISO power and higher CARS total scores across multiple posterior and temporal regions.

Although these findings highlight meaningful associations between ISO power, spindle dynamics and clinical features, they should not be interpreted as evidence of diagnostic or disorder-specific biomarkers. Prior work shows that stronger infraslow activity is associated with adaptive cognitive processes, such as enhanced spatial memory consolidation in healthy adults (Lecci et al. 2017), and that ISO power can be reduced in schizophrenia without corresponding relationships to symptom severity (Dimitriades et al. 2025). These studies indicate that ISO dynamics reflect broad thalamocortical and arousal-regulatory mechanisms rather than signatures unique to any specific disorder. In this context, our findings likely represent early developmental differences in cortical-thalamic coordination in ASD, and any biomarker implications require cautious and longitudinal validation.

The thalamocortical circuits are responsible for sleep spindles, where the precise spindle–SO coupling requires coordination of the thalamus and the cortex during NREM sleep (Clemente-Perez et al. 2017; Cumming et al. 2024; Lüthi 2014; Takata 2020). Prior structural and functional studies have suggested that the frontal cortical and thalamocortical pathways mature rapidly during early childhood and may follow atypical developmental trajectories in some children with ASD (Courchesne et al. 2011; Hazlett et al. 2005, 2011). The present finding of elevated SO-phase-dependent modulation of spindle frequency at F8 in the ASD group is therefore consistent with prior evidence of altered thalamocortical development in autism and may reflect early differences in the coordination of cortical and thalamic rhythms (Cerliani et al. 2015; Iidaka et al. 2019; Linke et al. 2018).

Although the group-level difference was confined to a single right frontal electrode, previous work has highlighted the importance of frontal spindle features during early development (D'Ambrosio et al. 2025). For example, studies in preschool-aged children have reported alterations in frontal spindle amplitude and ISA in ASD, suggesting that this region may be particularly sensitive to early neurodevelopmental divergence (D'Ambrosio et al. 2025). The current findings thus extend this literature by identifying a phase-dependent spindle characteristic that may help distinguish ASD from TD children during a critical developmental window.

Developmental effects were also observed independent of diagnostic group. Specifically, mean ISA per spindle at frontal sites F4 and F7 decreased with age, aligning with established developmental patterns showing age-related changes in spindle properties during infancy and early childhood (Scholle et al. 2007). These results support the notion that frontal circuits undergo rapid maturation in this age range and may represent a sensitive window for detecting both typical and atypical trajectories. Sex-stratified analyses further revealed that several EEG-clinical associations differed by sex and were primarily driven by strong negative correlations in females. Notably, in females, higher SO-phase-dependent spindle frequency modulation at F8 was associated with lower ADOS severity scores. These findings suggest that certain aspects of sleep microstructure may relate to clinical features in a sex-dependent manner, though the small number of females warrants cautious interpretation.

Both groups exhibited a visually identifiable peak near ~0.02 Hz, detectable even in children as young as 1 year old. This observation suggests that certain elements of ISO are robust features of early sleep physiology. Notably, the relative ISO topography in our cohort did not show the central-parietal predominance reported in older children and adults (Dimitriades et al. 2025; Lecci et al. 2017). Several developmental and methodological factors likely contribute to this discrepancy. First, our participants were between 1.1 and 5.1 years old, a developmental period during which large-scale cortical networks and thalamocortical connectivity are rapidly maturing, and electrophysiological signatures such as sigma and spindle-related dynamics are not yet fully stabilised (Jaramillo et al. 2023; McClain et al. 2016). Second, recordings were obtained during daytime naps following partial sleep deprivation, which typically yields shorter, developmentally variable mixtures of NREM stages, as ISO topography is known to vary with sleep-stage composition (Lázár et al. 2019). Finally, the limited sample size in this study cohort likely reduced the stability of channel-wise spectral estimates, particularly when analysed using sex-stratified subgroups. Together, these factors are likely to jointly contribute to the flatter scalp distribution of ISO power observed in the present study cohort.

When looking at the EEG-ASD clinical metric associations, the positive association between SO-phase-dependent spindle frequency modulation and better fine motor skills is unexpected since the spindle frequency modulation was higher in ASD at F8. On the other hand, the ISO strength showed spatially broad positive associations with CARS, that is, higher ASD severity. The result is consistent with recent imaging studies that demonstrated excessive CSF in the subarachnoid space in children with ASD, particularly over the frontal lobes, observable as early as 6 months of age and persisting into early childhood (Shen et al. 2018). In individuals with severe autism, the excessive extra-axial CSF and impaired CSF outflow may increase the mechanical and metabolic load on glymphatic clearance and may reflect compensatory infraslow vasomotor/CSF pumping. Meanwhile, because ISO is closely linked to vasomotor activity and CSF flow during sleep, stronger ISO power may represent an electrophysiological signature of altered CSF dynamics (Hauglund et al. 2025).

Our study has several limitations. First, the sample size was small, particularly among female participants with ASD. Given documented sex differences in clinical presentation and neurobiology in ASD, the limited number of female participants constrains the robustness and generalizability of our sex-specific findings. Second, the sleep recording was conducted during the day in an experimental setting, which could introduce differences from nighttime at-home conditions. Third, there is no external validation. An external study with the same age range is needed to replicate the findings. Another important future step is the establishment of normative developmental trajectories for ISO, stratified by age and sex.

5 | Conclusion

Overall, the findings highlight sleep EEG as a promising noninvasive tool for probing early autism mechanisms and advancing biomarker development to improve diagnosis and guide early intervention strategies.

Author Contributions

Kevin Liu: conceptualization, resources, project administration, software, validation, formal analysis, data curation, investigation, writing – original draft preparation, writing – review and editing, visualization. **Binbin Sun:** conceptualization, resources, project administration, methodology, data collection, investigation, writing – review and editing, funding acquisition. **Bryan K. Wang:** software, validation, formal analysis, data curation, writing – original draft preparation, writing – review and editing. **Jonathan Chen:** software, validation, formal analysis, data curation, writing – review and editing. **M. Brandon Westover:** writing – review and editing. **Fu-Ying Tian:** methodology, data collection, writing – review and editing. **Haoqi Sun:** conceptualization, resources, project administration, software, validation, formal analysis, data curation, investigation, writing – original draft preparation, writing – review and editing, visualization, supervision. **Xue-Jun Kong:** conceptualization, resources, project administration, investigation, writing – review and editing, supervision, funding acquisition.

Acknowledgements

The authors sincerely thank all the participating subjects and their parents for their valuable contributions.

Funding

This work was supported by General Projects of the Shenzhen Science and Technology Program, China (JCYJ20240813115124032, JCYJ20210324131211031), Shenzhen Maternity and Child Healthcare Hospital (FYA2022018), Sanming Project of Medicine in Shenzhen Municipality (SZSM201512009), Natural Science Foundation of Guangdong Province of China (2022A1515010617), Athinoula A. Martinos Center for Biomedical Imaging, Massachusetts General Hospital (233263), and Boston Children's Hospital (92436).

Conflicts of Interest

Dr. M. Brandon Westover is a co-founder, scientific advisor, and consultant for Beacon Biosignals and holds personal equity in the company. All other authors declare no conflicts of interest.

Data Availability Statement

The data that support the findings of this study are available from the corresponding author upon reasonable request.

References

American-Psychiatric-Association. 2013. *Diagnostic and Statistical Manual of Mental Disorders: DSM-5*. Vol. 5. 5th ed. American psychiatric association.

Arazi, A., G. Meiri, D. Danan, et al. 2019. "Reduced Sleep Pressure in Young Children With Autism." *Sleep* 43, no. 6: zsz309. https://doi.org/10.1093/sleep/zsz309.

Bastian, L., A. Samanta, D. R. de Paula, et al. 2022. "Spindle–Slow Oscillation Coupling Correlates With Memory Performance and Connectivity Changes in a Hippocampal Network After Sleep." *Human Brain Mapping* 43, no. 13: 3923–3943. https://doi.org/10.1002/hbm.25893.

Berry, R. B., R. Budhiraja, D. J. Gottlieb, et al. 2012. "Rules for Scoring Respiratory Events in Sleep: Update of the 2007 AASM Manual for the Scoring of Sleep and Associated Events: Deliberations of the Sleep Apnea Definitions Task Force of the American Academy of Sleep

Medicine." *Journal of Clinical Sleep Medicine* 8, no. 5: 597–619. https://doi.org/10.5664/jcsm.2172.

Campbell, I. G. 2009. "EEG Recording and Analysis for Sleep Research." *Current Protocols in Neuroscience* 49, no. 1: 10.2.1-10.2.19. https://doi.org/10.1002/0471142301.ns1002s49.

Cerliani, L., M. Mennes, R. M. Thomas, A. D. Martino, M. Thioux, and C. Keysers. 2015. "Increased Functional Connectivity Between Subcortical and Cortical Resting-State Networks in Autism Spectrum Disorder." *JAMA Psychiatry* 72, no. 8: 767–777. https://doi.org/10.1001/jamapsychiatry.2015.0101.

Clemente-Perez, A., S. R. Makinson, B. Higashikubo, et al. 2017. "Distinct Thalamic Reticular Cell Types Differentially Modulate Normal and Pathological Cortical Rhythms." *Cell Reports* 19, no. 10: 2130–2142. https://doi.org/10.1016/j.celrep.2017.05.044.

Courchesne, E., K. Campbell, and S. Solso. 2011. "Brain Growth Across the Life Span in Autism: Age-Specific Changes in Anatomical Pathology." *Brain Research* 1380: 138–145. https://doi.org/10.1016/j.brainres.2010.09.101.

Cumming, D., N. Kozhemiako, A. E. Thurm, C. A. Farmer, S. Purcell, and A. W. Buckley. 2024. "Spindle Chirp and Other Sleep Oscillatory Features in Young Children With Autism." *Sleep Medicine* 119: 320–328. https://doi.org/10.1016/j.sleep.2024.05.008.

D'Ambrosio, S., D. Gualandris, D. Caputo, et al. 2025. "Sleep Spindle Abnormalities in Preschool Children With Autism Spectrum Disability: Insights From Nap Polysomnography." *Autism Research* 18, no. 9: 1764–1774. https://doi.org/10.1002/aur.70087.

Dimitriades, M. E., E. Schumacher, J. Arudchelvam, et al. 2025. "The Infraslow Fluctuation of Sigma Power During Sleep in Young Individuals With Schizophrenia." *Schizophrenia Research* 285: 295–303. https://doi.org/10.1016/j.schres.2025.09.029.

Fjell, A. M., and K. B. Walhovd. 2025. "Sleep Patterns and Human Brain Health." *Neuroscientist* 31, no. 5: 483–498. https://doi.org/10.1177/10738584241309850.

Frankenburg, W. K., and J. B. Dodds. 1967. "The Denver Developmental Screening Test." *Journal of Pediatrics* 71, no. 2: 181–191. https://doi.org/10.1016/s0022-3476(67)80070-2.

Gao, R., and P. Penzes. 2015. "Common Mechanisms of Excitatory and Inhibitory Imbalance in Schizophrenia and Autism Spectrum Disorders." *Current Molecular Medicine* 15, no. 2: 146–167. https://doi.org/10.2174/1566524015666150303003028.

Gesell, A., and C. S. Amatruda. 1945. "Developmental Diagnosis." *Journal of Nervous and Mental Disease* 101, no. 1: 89.

Hauglund, N. L., M. Andersen, K. Tokarska, et al. 2025. "Norepinephrine-Mediated Slow Vasomotion Drives Glymphatic Clearance During Sleep." *Cell* 188, no. 3: 606–622.e17. https://doi.org/10.1016/j.cell.2024.11.027.

Hazlett, H. C., M. Poe, G. Gerig, et al. 2005. "Magnetic Resonance Imaging and Head Circumference Study of Brain Size in Autism: Birth Through Age 2 Years." *Archives of General Psychiatry* 62, no. 12: 1366–1376. https://doi.org/10.1001/archpsyc.62.12.1366.

Hazlett, H. C., M. D. Poe, G. Gerig, et al. 2011. "Early Brain Overgrowth in Autism Associated With an Increase in Cortical Surface Area Before Age 2 Years." *Archives of General Psychiatry* 68, no. 5: 467–476. https://doi.org/10.1001/archgenpsychiatry.2011.39.

Herrera, C. G., and L. Tarokh. 2024. "A Thalamocortical Perspective on Sleep Spindle Alterations in Neurodevelopmental Disorders." *Current Sleep Medicine Reports* 10, no. 2: 103–118. https://doi.org/10.1007/s40675-024-00284-x.

Iidaka, T., T. Kogata, Y. Mano, and H. Komeda. 2019. "Thalamocortical Hyperconnectivity and Amygdala-Cortical Hypoconnectivity in Male Patients With Autism Spectrum Disorder." *Frontiers in Psychiatry* 10: 252. https://doi.org/10.3389/fpsyt.2019.00252.

Jaramillo, V., S. F. Schoch, A. Markovic, et al. 2023. "An Infant Sleep Electroencephalographic Marker of Thalamocortical Connectivity Predicts Behavioral Outcome in Late Infancy." *NeuroImage* 269: 119924. https://doi.org/10.1016/j.neuroimage.2023.119924.

Jiang, C.-C., L.-S. Lin, S. Long, et al. 2022. "Signalling Pathways in Autism Spectrum Disorder: Mechanisms and Therapeutic Implications." *Signal Transduction and Targeted Therapy* 7, no. 1: 229. https://doi.org/10.1038/s41392-022-01081-0.

Kawahara, M., K. Kagitani-Shimono, K. Kato-Nishimura, et al. 2022. "A Preliminary Study of Sleep Spindles Across Non-Rapid Eye Movement Sleep Stages in Children With Autism Spectrum Disorder." *SLEEP Advances* 3, no. 1: zpac037. https://doi.org/10.1093/sleepadvances/zpac037.

Lai, M.-C., M. V. Lombardo, B. Auyeung, B. Chakrabarti, and S. Baron-Cohen. 2015. "Sex/Gender Differences and Autism: Setting the Scene for Future Research." *Journal of the American Academy of Child & Adolescent Psychiatry* 54, no. 1: 11–24. https://doi.org/10.1016/j.jaac.2014.10.003.

Lázár, Z. I., D.-J. Dijk, and A. S. Lázár. 2019. "Infraslow Oscillations in Human Sleep Spindle Activity." *Journal of Neuroscience Methods* 316: 22–34. https://doi.org/10.1016/j.jneumeth.2018.12.002.

Lecci, S., L. M. J. Fernandez, F. D. Weber, et al. 2017. "Coordinated Infraslow Neural and Cardiac Oscillations Mark Fragility and Offline Periods in Mammalian Sleep." *Science Advances* 3, no. 2: e1602026. https://doi.org/10.1126/sciadv.1602026.

Linke, A. C., R. J. J. Keehn, E. B. Pueschel, I. Fishman, and R.-A. Müller. 2018. "Children With ASD Show Links Between Aberrant Sound Processing, Social Symptoms, and Atypical Auditory Interhemispheric and Thalamocortical Functional Connectivity." *Developmental Cognitive Neuroscience* 29: 117–126. https://doi.org/10.1016/j.dcn.2017.01.007.

Lord, C., S. Risi, L. Lambrecht, et al. 2000. "The Autism Diagnostic Observation Schedule—Generic: A Standard Measure of Social and Communication Deficits Associated With the Spectrum of Autism." *Journal of Autism and Developmental Disorders* 30, no. 3: 205–223. https://doi.org/10.1023/a:1005592401947.

Lord, C., M. Rutter, and A. L. Couteur. 1994. "Autism Diagnostic Interview-Revised: A Revised Version of a Diagnostic Interview for Caregivers of Individuals With Possible Pervasive Developmental Disorders." *Journal of Autism and Developmental Disorders* 24, no. 5: 659–685.

Lüthi, A. 2014. "Sleep Spindles." *Neuroscientist* 20, no. 3: 243–256. https://doi.org/10.1177/1073858413500854.

Martin, N., M. Lafortune, J. Godbout, et al. 2013. "Topography of Age-Related Changes in Sleep Spindles." *Neurobiology of Aging* 34, no. 2: 468–476. https://doi.org/10.1016/j.neurobiolaging.2012.05.020.

McClain, I. J., C. Lustenberger, P. Achermann, J. M. Lassonde, S. Kurth, and M. K. LeBourgeois. 2016. "Developmental Changes in Sleep Spindle Characteristics and Sigma Power Across Early Childhood." *Neural Plasticity* 2016, no. 1: 3670951. https://doi.org/10.1155/2016/3670951.

McFayden, T. C., O. Putnam, R. Grzadzinski, and C. Harrop. 2023. "Sex Differences in the Developmental Trajectories of Autism Spectrum Disorder." *Current Developmental Disorders Reports* 10, no. 1: 80–91. https://doi.org/10.1007/s40474-023-00270-y.

Moore, M., V. Evans, G. Hanvey, and C. Johnson. 2017. "Assessment of Sleep in Children With Autism Spectrum Disorder." *Children* 4, no. 8: 72. https://doi.org/10.3390/children4080072.

Ng, T., E. Noh, and R. M. Spencer. 2025. "Bayesian Meta-Analysis Reveals the Mechanistic Role of Slow Oscillation-Spindle Coupling in Sleep-Dependent Memory Consolidation." *eLife* 13: RP101992. https://doi.org/10.7554/elife.101992.

Osorio-Forero, A., G. Foustoukos, R. Cardis, et al. 2025. "Infraslow Noradrenergic Locus Coeruleus Activity Fluctuations Are Gatekeepers

of the NREM–REM Sleep Cycle." *Nature Neuroscience* 28, no. 1: 84–96. https://doi.org/10.1038/s41593-024-01822-0.

Palmer, C. A., and C. A. Alfano. 2017. "Sleep and Emotion Regulation: An Organizing, Integrative Review." *Sleep Medicine Reviews* 31: 6–16. https://doi.org/10.1016/j.smrv.2015.12.006.

Peltola, M. E., M. Leitinger, J. J. Halford, et al. 2023. "Routine and Sleep EEG: Minimum Recording Standards of the International Federation of Clinical Neurophysiology and the International League Against Epilepsy." *Epilepsia* 64, no. 3: 602–618. https://doi.org/10.1111/epi.17448.

Purcell, S. M., D. S. Manoach, C. Demanuele, et al. 2017. "Characterizing Sleep Spindles in 11,630 Individuals From the National Sleep Research Resource." *Nature Communications* 8, no. 1: 15930. https://doi.org/10.1038/ncomms15930.

Scholle, S., G. Zwacka, and H. C. Scholle. 2007. "Sleep Spindle Evolution From Infancy to Adolescence." *Clinical Neurophysiology* 118, no. 7: 1525–1531. https://doi.org/10.1016/j.clinph.2007.03.007.

Schopler, E., R. J. Reichler, R. F. DeVellis, and K. Daly. 1980. "Toward Objective Classification of Childhood Autism: Childhood Autism Rating Scale (CARS)." *Journal of Autism and Developmental Disorders* 10, no. 1: 91–103. https://doi.org/10.1007/bf02408436.

Shaw, K. A., S. Williams, M. E. Patrick, et al. 2025. "Prevalence and Early Identification of Autism Spectrum Disorder Among Children Aged 4 and 8 Years—Autism and Developmental Disabilities Monitoring Network, 16 Sites, United States, 2022." *MMWR Surveillance Summaries* 74, no. 2: 1–22. https://doi.org/10.15585/mmwr.ss7402a1.

Shen, M. D., C. W. Nordahl, D. D. Li, et al. 2018. "Extra-Axial Cerebrospinal Fluid in High-Risk and Normal-Risk Children With Autism Aged 2–4 Years: A Case-Control Study." *Lancet Psychiatry* 5, no. 11: 895–904. https://doi.org/10.1016/s2215-0366(18)30294-3.

Souders, M. C., S. Zavodny, W. Eriksen, et al. 2017. "Sleep in Children With Autism Spectrum Disorder." *Current Psychiatry Reports* 19, no. 6: 34. https://doi.org/10.1007/s11920-017-0782-x.

Sun, H., E. Ye, L. Paixao, et al. 2023. "The Sleep and Wake Electroencephalogram Over the Lifespan." *Neurobiology of Aging* 124: 60–70. https://doi.org/10.1016/j.neurobiolaging.2023.01.006.

Takata, N. 2020. "Thalamic Reticular Nucleus in the Thalamocortical Loop." *Neuroscience Research* 156: 32–40. https://doi.org/10.1016/j.neures.2019.12.004.

Tononi, G., and C. Cirelli. 2006. "Sleep Function and Synaptic Homeostasis." *Sleep Medicine Reviews* 10, no. 1: 49–62. https://doi.org/10.1016/j.smrv.2005.05.002.

Walker, M. P., and R. Stickgold. 2004. "Sleep-Dependent Learning and Memory Consolidation." *Neuron* 44, no. 1: 121–133. https://doi.org/10.1016/j.neuron.2004.08.031.

Werling, D. M., and D. H. Geschwind. 2013. "Sex Differences in Autism Spectrum Disorders." *Current Opinion in Neurology* 26, no. 2: 146–153. https://doi.org/10.1097/wco.0b013e32835ee548.

Supporting Information

Additional supporting information can be found online in the Supporting Information section. **Figure S1:** Performance of automated spindle detection against human annotation. (a) Histogram illustrating the distribution of the quality index for 786 randomly selected spindle candidates. Blue bars represent events labelled as 'not spindle', and red bars represent events labelled as 'spindle' by the human annotator. The dashed vertical red line indicates the optimal quality index cutoff (0.53), determined by Youden's *J* statistic from the Receiver Operating Characteristic (ROC) analysis. (b) ROC curve comparing automated spindle detection based on the quality index with human annotation, with an area under the ROC (AUROC) of 0.69. The optimal operating point (red circle), based on Youden's index, yields a sensitivity (true positive rate) of 0.71 and a specificity of 0.58 (false positive rate of 0.42). (c) Precision-Recall curve illustrating performance, with an area under the curve (AUPRC) of 0.54. The optimal operating point (red circle) corresponds to a precision of 0.43 and a recall of 0.71. (d) Confusion matrix at the optimal quality index cutoff, comparing human annotation (rows) with automated spindle detection (columns). The corresponding F1 score was 0.54 and Cohen's kappa coefficient was 0.24. Colour intensity indicates the sample size within each cell. **Figure S2:** Topographical distribution of age-related effects on spindle microstructure features. Regression coefficients (β values) from models predicting spindle features as a function of age, adjusted for group and sex. (a) Mean integrated spindle activity (ISA) per spindle. (b) Spindle density (count per minute). (c) Mean spindle frequency (FFT-derived). Channels with statistically significant effects (after multiple comparison correction) are highlighted in yellow. Red shading indicates stronger effects in the positive direction; blue shading indicates stronger negative effects. **Figure S3:** Channel-level ISO spectral power is shown across frequency for the youngest individuals in each group. (a) TD subjects aged at 1.05 years; (b) ASD subjects aged at 1.06 years. Each panel represents a single subject, with coloured lines indicating power from individual EEG channels. **Figure S4:** Sex-stratified scatterplots of significant EEG-clinical correlations in ASD. Shown are all EEG-clinical feature pairs with significant correlations in at least one sex. **Table S1:** Correlations between relative ISO band power (0.005–0.03 Hz) across scalp EEG channels and clinical measures in males with ASD.